RSC Advances

ROYAL SOCIETY OF CHEMISTRY

www.rsc.org/advances

RSC Advances

RSCPublishing

ARTICLE

Malachite green Adsorption onto Fe_3O_4@SiO_2-NH_2: Isotherms, Kinetic and Process Optimization

Cite this: DOI: 10.1039/x0xx00000x

Ling Sun, Shuchao Hu, Hongmei Sun, Huiling Guo, Hongda Zhu, Mingxing Liu and Honghao Sun*

Received ooth January 2012,
Accepted ooth January 2012

DOI: 10.1039/x0xx00000x

www.rsc.org/

Higher environmental standards have made the removal of dye from water an important problem for many industrialized countries. Among the removed methods, magnetic adsorbents have received much attention for adsorption of dyes. In this paper, a novel magnetic adsorbent with an amino-modified SiO_2-coated Fe_3O_4 magnetite was prepared. The analysis of Fe_3O_4@SiO_2-NH_2 provided that the nanoparticles were uniform with the diameter of 90 nm. The difference of Fe_3O_4@SiO_2-NH_2 and Fe_3O_4@SiO_2 on the adsorption behaviour of malachite green was studied. The Fe_3O_4@SiO_2-NH_2 showed a good capacity for the adsorption of malachite green comparing with the Fe_3O_4@SiO_2, which shown to be influenced by the initial concentration and pH. Under the optimal conditions, the removal efficiency of malachite green was over 90% by the Fe_3O_4@SiO_2-NH_2, while using the Fe_3O_4@SiO_2 efficiency was below 60%. The experimental data fit well with the Freundlich isotherm and the pseudo-second-order kinetic model. In further applications, real samples were treated by the Fe_3O_4@SiO_2-NH_2 nanoparticles. All the results demonstrated that the Fe_3O_4@SiO_2-NH_2 nanoparticles could be a promising and effective adsorbent.

1 Introduction

The rapid growth of different chemical industries has been identified as among the main causes of environmental pollution.[1,2] Many chemical industries such as paper, plastics, cosmetics, leather, printing, pharmaceuticals and textile use dyes for colouring their products and release the various types of dyes into water bodies, which generate wastewater with characteristically high in colour and organic content.[3,4] The process of discharging not only affects their aesthetic nature but also interferes with the transmission of sunlight into streams and therefore reduces photosynthetic action.[5] Furthermore, coloured wastes containing dyes exhibit toxic effects towards microbial populations and can be toxic and carcinogenic to mammals. Removal of many dyes by conventional methods is hard since these are resistant to aerobic digestion and are stable to light and oxidizing agents.[6] The shortage of water resource offers us a new assignment to decolorize the dying effluent, without disturbing the quality of water to make it reusable for various industrial and agricultural applications.[7]

Malachite Green (MG), a basic dye, has a wide application which includes the aquaculture, commercial fish hatchery and animal husbandry as an antifungal therapeutic agent, while for human it is used as antiseptic and fungicidal.[8,9] Despite its widely use, malachite green cause diseases like eye burns, fast breathing, profuse sweating and cancer of different parts of the body.[10,11] Due to its health hazard concerns, malachite green is banned in Europe, United States and Canada.[12] Although malachite green has adverse effects in humans, actually malachite green has been illegally used in many parts of the word for various economic or industrial purposes. Therefore, the treatment of effluents containing malachite green is of great interest owing to its harmful impacts on receiving waters.

A wide range of methods including filtration, centrifugation, electro-coagulation, adsorption, membrane-based separation, oxidative degradation and biochemical degradation have been utilized for removing dyes waste water.[13] Among them, magnetic separation has gained favours in recent years due to the super paramagnetic property, as they are attracted to magnetic field, but after removal of magnetic field, no extra magnetism is retained.[14,15] Fe_3O_4 nanoparticle is the first choice for magnetic adsorption because of the low cost, simplicity of design, easy operation and good biocompatibility.[16] As well as, it is not hard to imagine that the Fe_3O_4 nanoparticle that used sorbent can be recycled easily from environment using a magnetic field. This is very important for the industrial application to avoid secondary pollution in wastewater treatment.[17] However, several inevitable problems are contacted with the Fe_3O_4 nanoparticle, such as their intrinsic instability over long periods due to their tendency to aggregate in order to reduce their surface energy, as well as the ease oxidation in air.[18] The aggregation of magnetic nanoparticles can significantly decrease their interfacial area, thus resulting in the loss of magnetism and dispersibility.[19] Silica nanoparticles are characteristic of large surface area, easy preparation by sol-gel method, easy functionalization and good stability in water.[20] To enhance the adsorption capacity of Fe_3O_4 nanoparticle, silica is used to coat on the Fe_3O_4 nanoparticles surface.[21] Through this approach, the core-shell structured Fe_3O_4@SiO_2 nanoparticle

can retain the super paramagnetic properties and be stable in water as well as easily functional with other group.

The removal of malachite green using the magnetic adsorbents with modified by the anionic groups like carboxyl and hydroxyl have been studied extensively.[22] Almost all these magnetic adsorbents showed low removal efficiency, due to high stable of the magnetic adsorbents in the water caused by the electrostatic repulsion between adsorbents. Nevertheless, the present study overcomes these drawbacks by utilizing surface modification of Fe_3O_4 with SiO_2 and 3-Aminopropyltriethoxysilane (APTES) for efficient removal of the malachite green. To the best of our knowledge, little work has been done on the removal of malachite green by the Fe_3O_4@SiO_2-NH_2. The pH effect, adsorption isotherm, adsorption kinetics, and the application of this magnetic adsorbent were studied.

2 Experimental

2.1 Materials

3-Aminopropyltriethoxysilane (APTES) was purchased from Sigma Aldrich. All chemicals were purchased from Sinopharm Chemical Reagents Company and used without further purification unless otherwise stated. Deionized water (18.4 MΩ cm) used for all experiments was obtained from a Milli-Q system (Millipore, Bedford, MA).

2.2 Preparation of Fe_3O_4 nanospheres

The magnetite nanoparticles were synthesized following the conventional co-precipitation method with slight modification.[23] Briefly, $FeSO_4 \cdot 7H_2O$ (200 mg, 0.7 mmol) and $FeCl_3 \cdot 6H_2O$ (400 mg, 1.4 mmol) were mixed with a magnetic stirrer in a 100 mL flask containing 20 mL of oxygen free deionized water. Ultrapure N_2 gas (99.999%, Wuhan Special Gas Inc., China) was used to remove oxygen and create an oxygen free condition during the synthesize process. The solutions were heated to 40°C with a digital heating circulating water bath (Kunshan Biotechnology Ltd., China). Ammonium hydroxide (28-30%) was then added to the solutions drop by drop until the pH reached around 10, under which conditions the black precipitate formed. The solutions were heated to 70°C within 10mins. Citric acid monohydrate (160 mg, 0.7 mmol) was added to the solutions. The mixture was stirred at 70°C for 50mins and then cooled to room temperature. The black precipitate was collected by magnetic decantation and repeatedly washed with deionized water until the washings were neutral. The product was dispersed to 10 mL water and separated by centrifugation at 6000 rpm for 30mins.

2.3 Preparation of Fe_3O_4@SiO_2 nanospheres

Core-shell structured Fe_3O_4@SiO_2 was fabricated by a modified *Stöber* method.[24,25] Typically, 5 mL of the above solution containing Fe_3O_4 (2.5 mg/mL) was mixed with 40 mL of ethanol and 5 mL of deionized water, followed by adding 0.032 mL of tetraethyl orthosilicate (TEOS). After the suspension was stirred for 15mins, 1 mL of $NH_3 \cdot H_2O$ was added drop wise and further reacted for 7h. Finally, the product was washed with ethanol and deionized water several times by centrifugation at 11000 rpm for 30mins. Finally the Fe_3O_4@SiO_2 was dispersed to 10 mL water.

2.4 Preparation of Fe_3O_4@SiO_2-NH_2 nanospheres

The preparation of Fe_3O_4@SiO_2 (10 mL) was added in 20 mL of ethanol, stirring for 10mins at room temperature. 0.003 mL APTES and 0.01 mL TEOS were then added to the solutions and further reacted for 7h. The black precipitate was collected by magnetic decantation and repeatedly washed with deionized water. Finally it was dispersed to 10 mL water.

2.5 Dye adsorption

Dyes removal efficiency was calculated by measuring the dye concentration before and after adsorption. The adsorbents were added to the dye solution and incubated at room temperature for 2 hours with shaking. At the end of adsorption, the suspension was separated by a magnet. The dye concentrations were determined by UV-vis spectroscopy (Scheme 1).[26]

2.6 Dye desorption

In order to access the utility of the adsorbent, desorption experiments were conducted. The initial concentration of malachite green solutions and Fe_3O_4@SiO_2-NH_2 were 10 mg/L and 100 mg/L, respectively. After adsorption for 40mins, the adsorbent was magnetically separated from the solution and then washed gently with deionized water. The collected malachite green-adsorbed Fe_3O_4@SiO_2-NH_2 was treated by adjusted pH to 3 by adding hydrochloric acid. The contact time of desorption process was set to be 40mins. At the end of desorption, the suspension was separated by a magnet. The dye concentrations were determined by UV-vis spectroscopy. The adsorption-desorption cycle was repeated four times by using the same Fe_3O_4@SiO_2-NH_2 that was washed repeatedly with deionized water until the effluent was neutral before the next cycle. [27]

2.7 Characterization

Powder X-ray diffraction (XRD) patterns were obtained using Bruker D8 ADVANCE diffraction meter (Germany). Samples were scanned in the range of diffraction angles 2θ=10-80° at a rate of 2° min^{-1} with a step width of 0.02° using Cu Kα radiation at λ=0.154 nm operating at 40 kV and 40 mA. Hydrodynamic diameter (Dh) and Zeta potential measurements were conducted by dynamic light scattering (DLS) with a Malvern Zetasizer Nano ZS90 (Malvern, UK) instrument using He-Ne laser at a wavelength of 632.8nm. Fourier transform infrared spectra (FT-IR) were recorded on a Magna550 (Nicolet, U.S.A.) spectrometer. Spectra were scanned over the range 400-4000 cm^{-1}. All of the dried samples were mixed with KBr and then compressed to form pellets. The transmission electron microscopy (TEM) images were taken on a JEM-2100F transmission electron microscope at an accelerating voltage of 200 kV. UV-vis spectra were recorded on a SHIMADZU UV-1800 UV-vis spectrophotometer (Japan).

3 Results and discussion

3.1 Structural and Morphological Characterization

The Fe_3O_4 particles were prepared via a co-precipitation method as described above. To obtain the structural information of Fe_3O_4 and Fe_3O_4@SiO_2, XRD characterization was conducted. Six diffraction lines (Figure 1a) were observed in the representative XRD pattern of Fe_3O_4 at 2θ=30.3°, 35.6°, 43.4°, 53.4°, 57.9° and 62.7°. These diffraction lines could be assigned to the (220), (311), (400), (422), (511) and (440)

reflections, respectively, of the pure cubic spinel crystal structure of Fe_3O_4 with cell constant α=8.34Å (JCPDS card No.19-0629).[28] The phase of the Fe_3O_4@SiO_2 was characterized by XRD (Figure 1b). While the broad peak at 2θ=15-29° could be ascribed to amorphous silica, the remainder of the peaks corresponded to the magnetite core phase of Fe_3O_4@SiO_2 (similar to Figure 1a).[29]

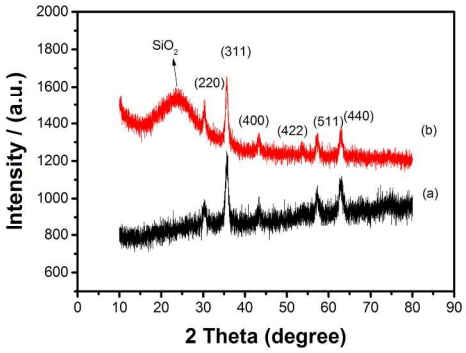

Figure 1 XRD patterns of (a) Fe_3O_4, (b) Fe_3O_4@SiO_2.

FT-IR spectroscopy was performed to confirm the surface chemistry of the magnetic nanoparticles in the range of 4000-500cm^{-1} (Figure 2). The peaks at 558cm^{-1} and 1630cm^{-1} appear in all the IR spectra, which were characteristic of Fe-O vibrations within the magnetic core and the stretching of the solvent hydroxyl, respectively.[30] After silica being coated, the main absorption bands associated with Si-O bending and Si-O-Si bending were observed at 793cm^{-1} and 451cm^{-1}, respectively.[31] Another characteristic signal 1091cm^{-1} was attributable to asymmetric Si-O-Si vibration or Si-O-Fe stretching vibration in the silica shell. These absorption bands clearly demonstrated SiO_2 coating of the Fe_3O_4 surface.[32,33] The stretching and bending vibrations of amino groups were detected at 1550, 1480 and 647cm^{-1}, which suggested that amino groups have been anchored on the surface of silica coating. Successful functionalization of amino propyl on silica coating was further confirmed by the presence of C-H stretching vibration observed at 2800~3025cm^{-1}.[4]

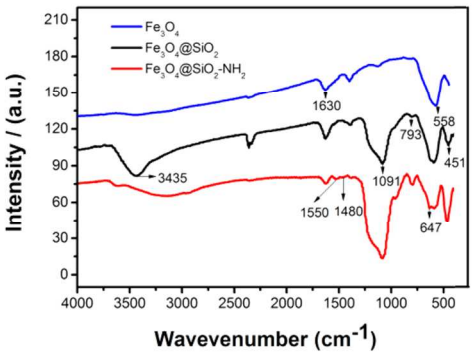

Figure 2 FT-IR spectrum of Fe_3O_4, Fe_3O_4@SiO_2 and Fe_3O_4@SiO_2-NH_2.

The morphology and size of the nanoparticles were investigated by TEM imaging (Figure 3). The mean diameter of Fe_3O_4, Fe_3O_4@SiO_2 and Fe_3O_4@SiO_2-NH_2 (Figure S1B-D) was estimated to be 15±2.3nm, 80±3.7nm, and 90±3.3nm, respectively. It is clear that the Fe_3O_4 were well coated with a silica layer. The number of the internal Fe_3O_4 sphere was estimated to be around 8 (Figure S2).

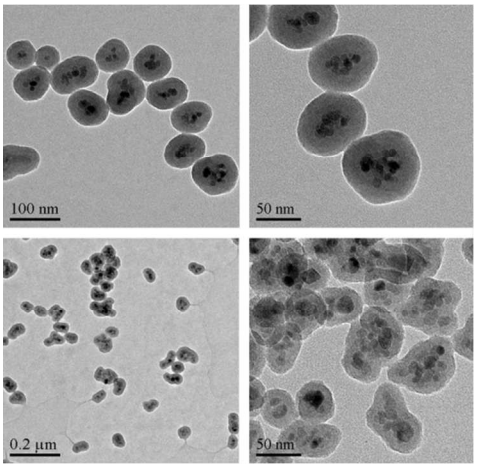

Figure 3 TEM images of Fe_3O_4@SiO_2 (up) and Fe_3O_4@SiO_2-NH_2 (down).

Dynamic light scattering measurements showed that the hydrodynamic diameter of Fe_3O_4, Fe_3O_4@SiO_2 and Fe_3O_4@SiO_2-NH_2 was 60nm, 95nm and 123nm, respectively. The difference size of nanoparticles between TEM and DLS could be reasoned by the aggregation of nanoparticles in water. The hydrodynamic diameter was bigger than that of dry state. The magnetic nanoparticles were uniform and the Polidispersity Index (PDI) of all samples was less than 0.2. Zeta potential of Fe_3O_4@SiO_2 was -28.1mV (Figure S3II). After amino functionalization, the zeta potential of Fe_3O_4@SiO_2-NH_2 increased to 36.3mV (Figure S3III) indicated that amino was successfully bounded to nanoparticles surface.

3.2 Adsorption properties

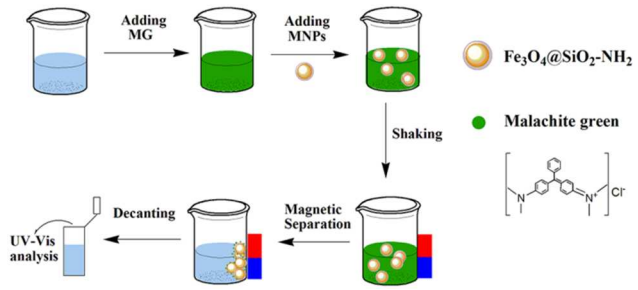

Scheme 1 Schematic illustration of the adsorption process for the malachite green using Fe_3O_4@SiO_2-NH_2.

3.2.1 Effect of Fe_3O_4@SiO_2-NH_2 and Fe_3O_4@SiO_2 Dosage.

Adsorbent dosage is an important parameter in adsorption process. It significantly influences the removal of adsorbate species.[34] The effects of Fe_3O_4@SiO_2-NH_2 and Fe_3O_4@SiO_2 dosage on the adsorption of malachite green were investigated at 25±1°C by varying the amount of adsorbent from 12 mg/L to 150 mg/L while keeping the concentration of malachite green solution constant (10 mg/L) in two hours.

Figure 4(a) displayed the percentage removal of malachite green versus the amount of adsorbent.[35] (Figure S4 in the ESM showed the typical UV-vis absorption of the malachite green using the Fe_3O_4@SiO_2-NH_2 and Fe_3O_4@SiO_2). Based on the

results in Figure 4, the removal of malachite green acquired a maximum and became steady thereafter with higher Fe_3O_4@SiO_2-NH_2 amount. This could be attributed to increased sorbent surface area and availability of more adsorption sites, while the steady was due to utilization of all malachite green available to the adsorption at higher concentration of Fe_3O_4@SiO_2-NH_2.[36,37] The optimum dosage of the Fe_3O_4@SiO_2-NH_2 was found to be 100 mg/L. Under the optimal conditions, the removal efficiency of malachite green was 91% by the Fe_3O_4@SiO_2-NH_2, while using the Fe_3O_4@SiO_2 efficiency was 57%. Therefore, Fe_3O_4@SiO_2-NH_2 had a better removal effect than Fe_3O_4@SiO_2.

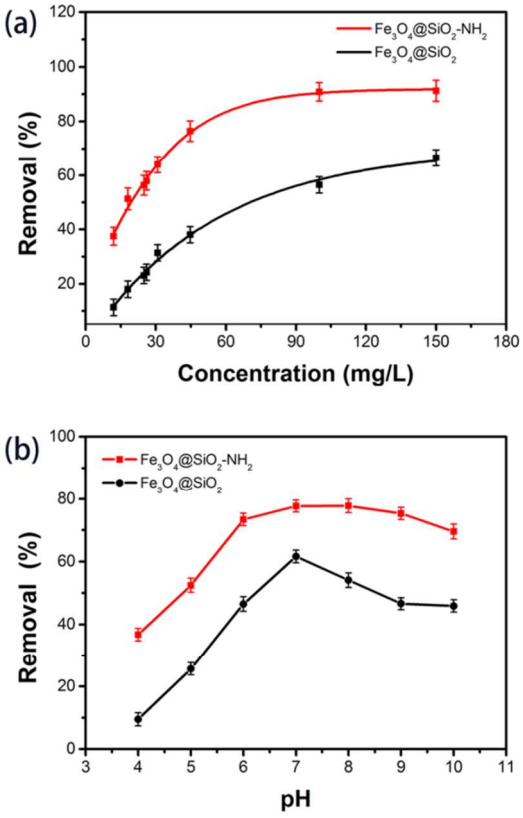

Figure 4(a) The removal of malachite green at different concentrations of Fe_3O_4@SiO_2 and Fe_3O_4@SiO_2-NH_2. (b) Effect of pH on the removal efficiency. The concentration of the adsorbent was 100mg/L and the initial concentration of dye solution was 10 mg/L.

3.2.2 Effect of pH - adsorption mechanism

Initial pH of dye can influence the adsorption of it on the surface of adsorbent.[38-40] In the present study, pH 4-10 were used to observe the better adsorption with initial concentration of malachite green 10 mg/L with 100 mg/L Fe_3O_4@SiO_2-NH_2 and Fe_3O_4@SiO_2 as adsorbent dosage.

Figure 4(b) showed the dye removal efficiency at various pH values (The UV-vis absorption of the malachite green removal efficiency using Fe_3O_4@SiO_2-NH_2 and Fe_3O_4@SiO_2 at various pH values were showed in Figure S5). Owing to the chemical structure of malachite green, the dye molecule was strongly positively charged over the whole pH range. The Z-potential value of Fe_3O_4@SiO_2-NH_2 and Fe_3O_4@SiO_2 varying with pH was shown in Figure S6. The isoelectric point of Fe_3O_4@SiO_2-NH_2 was found to be 7.5. With rising solution pH, the zeta potentials of Fe_3O_4@SiO_2-NH_2 and Fe_3O_4@SiO_2 continuously decreased. Below the possible interactions for different pH conditions were explained.[41] In the case of Fe_3O_4@SiO_2-NH_2, the removal of malachite green showed an improvement with the increase of the solution pH. In particular, the malachite green removal was 36%, 52% and 77% at pH 4, 5 and 6, respectively. At acidic media (pH 4), the amino groups of Fe_3O_4@SiO_2-NH_2 were fully protonated, and the electrostatic interaction between nanoparticles and malachite green was week, which caused the low removal efficiency. At neutral conditions (pH 7), even the whole Fe_3O_4@SiO_2-NH_2 was positively charged, the hydroxyl groups of silica were still negatively charged. The electrostatic attraction between negatively charged hydroxyl groups and positively charged malachite green benefitted the adsorption of malachite green. Meanwhile the positively charged ammonium group of Fe_3O_4@SiO_2-NH_2 and negatively charged hydroxyl groups could cause attraction between nanoparticles, which helped to magnetic separation. In contrast, in neutral medium, the Fe_3O_4@SiO_2 were fully negatively charged, which made the nanoparticles too stable in aqueous solution and difficulties to be separated by magnetic separation. Due to the above mentioned reasons, the Fe_3O_4@SiO_2-NH_2 had better malachite green removal efficiency than that of Fe_3O_4@SiO_2. The mechanism of adsorption interactions was shown in the Scheme 2.

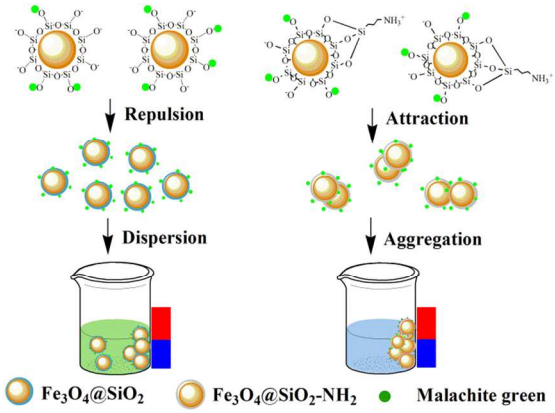

Scheme 2 Schematic illustration of the adsorption process for the malachite green using Fe_3O_4@SiO_2-NH_2 and Fe_3O_4@SiO_2 at pH 7.

3.2.3 Effect of surfactant and ionic strength

The high ionic strength may significantly affect the performance of the adsorption process.[42] Effect of 0.02, 0.04, 0.06, 0.08, 0.1, 0.15 and 0.2M NaCl solutions on adsorption of malachite green on Fe_3O_4@SiO_2-NH_2 was studied. The concentration of the adsorbent was 100 mg/L and the initial concentration of malachite green solution was 10 mg/L. Figure 5 indicated that with an increase in salt concentration, adsorption efficiency gradually decreased. This could be attributed to the competitive effect between malachite green and Na^+ ions for the available adsorption sites. As the ionic strength increased, the activity of malachite green and the active sites for adsorption decreased. Therefore, the removal of malachite green decreased.[43]

The effect of surfactant on the adsorption ability of Fe_3O_4@SiO_2-NH_2 was shown in Figure S7. The dye removal efficiency by Fe_3O_4@SiO_2-NH_2 was studied in the presence of cationic surfactant (Cetyl Trimethyl Ammonium Bromide,

CTAB, 0.02M), anionic surfactant (Sodium Dodecyl Sulfonate, SDS, 0.02M) and non-ionic surfactant (Tween-20, 0.02M). The results of the experiment showed that the SDS and Tween-20 had little influence in removal efficiency of malachite green, while the dye removal much affected by the CTAB due to the competitive effect between malachite green and CTAB for the available adsorption sites.

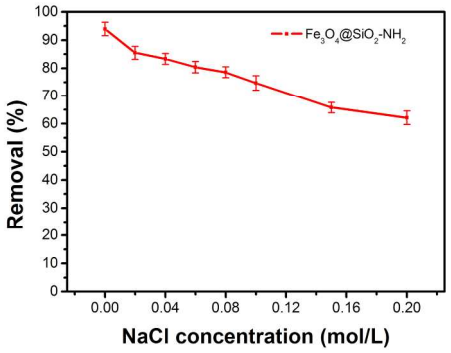

Figure 5 The effect of NaCl concentration on adsorption of malachite green on Fe_3O_4@SiO_2-NH_2.

3.2.4 Adsorption isotherm

An adsorption isotherm expresses the relationship between the mass of dye adsorbed at a given temperature under equilibrium conditions per unit mass of adsorbent (qe, mg/mg) and the liquid phase dye concentration (Ce, mg/L). They were very useful in providing information about adsorption mechanisms, surface properties and affinity of an adsorbent towards an adsorbate.[20] For the equilibrium study of adsorption of malachite green onto Fe_3O_4@SiO_2-NH_2 and Fe_3O_4@SiO_2, the experiments were conducted at different adsorbent concentrations (12-150 mg/L) (Figure 6a).[43] The experimental data obtained were evaluated by Freundlich isotherm models (Figure 6b).[44] The Freundlich isotherm was represented by Eq. (1):

$$\log q_e = \log K + \frac{\log C_e}{n} \qquad (1)$$

C_e is the concentration of dye under equilibrium condition (mg/L), q_e is the amount of dye adsorbed at equilibrium (mg/mg), K is the Freundlich constant denoting adsorption capacity (mg/mg) and n is the heterogeneity factor which is related to the intensity of adsorption (mg/L). A linear plot of $\log q_e$ versus $\log C_e$ provides the K and n values.[35]

Figure 6b demonstrated that Freundlich isotherm model was a better mathematical fit to experimental data, which suggested the adsorbent surface was heterogeneous in nature. The adsorption constants evaluated from the isotherms for Fe_3O_4@SiO_2-NH_2 and Fe_3O_4@SiO_2 were listed in Table 1. The n value of Fe_3O_4@SiO_2-NH_2 obtained from the Freundlich isotherm was larger than unity, indicated that the interaction force between the dyes and Fe_3O_4@SiO_2-NH_2 was strong.[26]

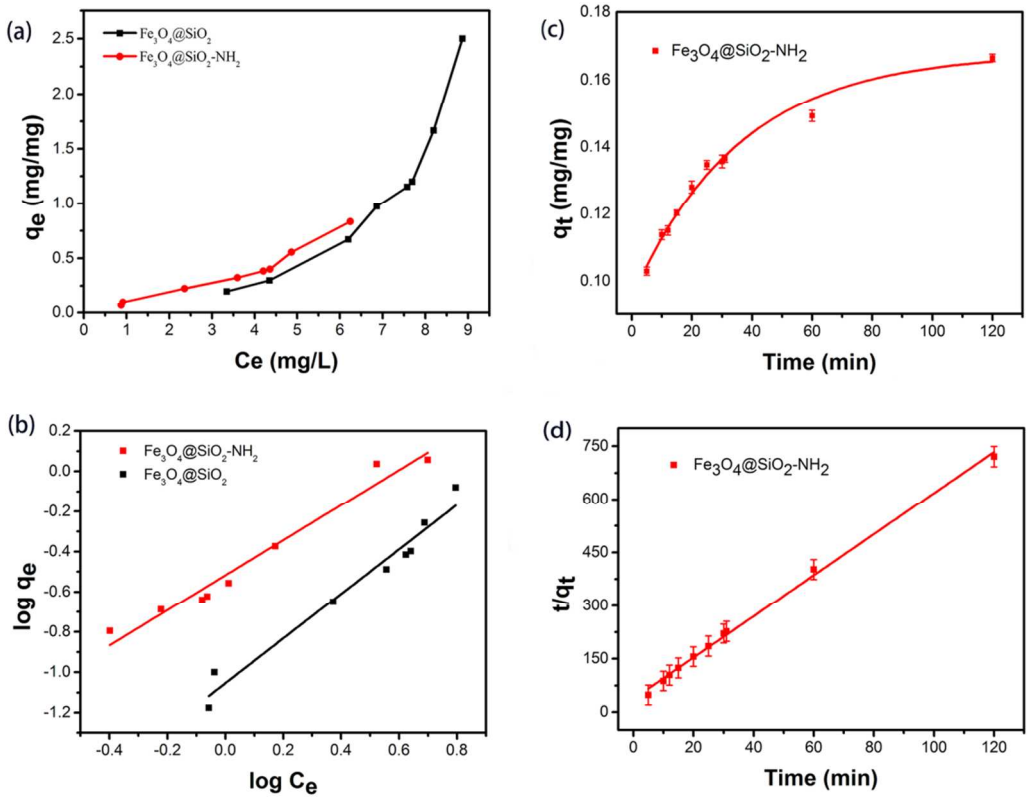

Figure 6(a) Adsorption isotherms of malachite green on the Fe_3O_4@SiO_2-NH_2 and Fe_3O_4@SiO_2 (temperature 25°C, pH 7). (b) Freundlich isotherms for malachite green on the Fe_3O_4@SiO_2-NH_2 and Fe_3O_4@SiO_2. Kinetic adsorption data plots for malachite green: (c) plot of removal rate q_t vs. t and (d) the transformed rate plot t/q_t vs. t. The initial concentration of dye solutions was 10mg/L and Fe_3O_4@SiO_2-NH_2 was 100 mg/L.

RSC Advances RSCPublishing

ARTICLE

Table 1 Freundlich isotherm constants and their correlation coefficients

	Freundlich	
	Fe_3O_4@SiO_2	Fe_3O_4@SiO_2-NH2
K (mg/mg)	0.349±0.035	0.596±0.027
n (mg/L)	0.902±0.043	1.140±0.036
R^2	0.96 ±0.051	0.96 ±0.042

3.2.5 Adsorption Kinetics

The adsorption efficiency depends well on contact time. The pseudo-second-order kinetics model was used to assess the mechanism of adsorption.[45]

Figure 6c showed the data for adsorption of malachite green solutions by Fe_3O_4@SiO_2-NH_2 at different time intervals. It was clear from this figure that the rate of adsorption was very fast in the initial stages and after equilibrium. For the first 40mins, the removal rate of malachite green was increased to 80%, suggested that Fe_3O_4@SiO_2-NH_2 had fast adsorption kinetics towards dye solutions. The kinetic data were analysed using pseudo-second order kinetics, which was based on the assumption that chemisorption was the rate determining step, and could be expressed as Eq. (2):

$$\frac{t}{q_t} = \frac{1}{(K_2 q_e)^2} + \frac{t}{q_e} \qquad (2)$$

Where q_e is the adsorption capacity at equilibrium and q_t is the loading of dye at time t. The parameter k_2 (g/(mg·min)) represents the pseudo-second-order rate constant for the kinetic model. The slope and intercept of the linear plot of t/q_t against t yield the values of q_e and k_2. Additionally, the initial adsorption rate V_0 (mg/(mg·min)) can be determined from Eq. (3):

$$V_0 = K_2 {q_e}^2 \qquad (3)$$

The c plots of t/q_t versus t are given in Figure 6d and the parameters of q_e (mg/g), k_2 (g/(mg·min)), V_0 (mg/(g·min)) and R^2 are shown in Table 2. The large correlation coefficients (R^2>0.96) suggest that dye uptake by Fe_3O_4@SiO_2-NH_2 follows the pseudo-second-order kinetic model.[26]

Table 2 Rate constants and correlation coefficients of the pseudo-second-order kinetic model.

		Fe_3O_4@SiO_2-NH_2
q_e	(mg/mg)	0.173±0.010
K_2	(mg/mg·min)	0.944±0.059
V_0	(mg/mg·min)	0.028±0.008
R^2		0.96±0.024

3.3 Desorption study

Good desorption performance of an adsorbent that can reduce the cost of treatment process. To investigate the reusability of the adsorbent, the absorption-desorption cycle was repeated four times by adjusted pH to 3 by adding hydrochloric acid. Figure 7 showed that the removal efficiency of dyes was still over 60% after reuse in five cycles, indicated that the as-prepared adsorbent had good reusability.

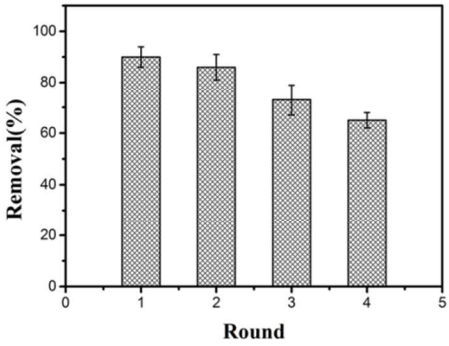

Figure 7 Recycling of Fe_3O_4@SiO_2-NH_2 in the removal of dyes. The initial concentration of malachite green solutions was 10 mg/L and that of Fe_3O_4@SiO_2-NH_2 was 100 mg/L.

3.4 Applications

In order to assess whether the new adsorbent developed here was suitable for practical applications, the malachite green from samples of different sources were treated using the excessive amounts of Fe_3O_4@SiO_2-NH_2. The different sources included local fishpound water, local industrial waste water and river water collected from Yangtze River in China. The results showed that malachite green residues in all samples were below the detectable level, indicated that these samples were practically free of malachite green. These worked samples were then spiked using standard amounts of malachite green to assess the removal effect. The concentration of malachite green was 10 mg/L and that of Fe_3O_4@SiO_2-NH_2 was 100 mg/L. The results showed that river water and fishpond water samples had little interference with the Fe_3O_4@SiO_2-NH_2, suggested that this new adsorbent was suitable for removal of dyes from real water (Figure 8).[26] While the industrial waste water sample showed not very well removal efficiency, it was likely to be due to the influence of the salt concentration. These results motivated us to broaden the utility of magnetic adsorbent (Fe_3O_4@SiO_2-NH_2) for dyes from industrial waste water. This work will be investigated and discussed in future.

In addition, Fe_3O_4@SiO_2-NH_2 also showed excellent removal efficiency for other dye pollutants including crystal violet and methylene blue in Yangtze River water, suggesting that the as-proposed method should be a general one for the removal of dye pollutants (Figure S8).

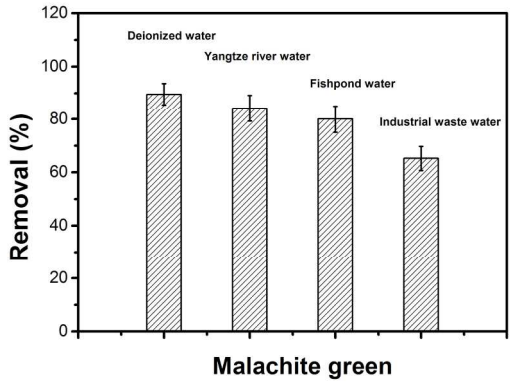

Figure 8 The removal efficiency of malachite green in different water samples. The initial concentration of malachite green and Fe_3O_4@SiO_2-NH_2 was 10 mg/L and 100 mg/L, respectively.

4 Conclusions

A simple method has been developed for preparing Fe_3O_4@SiO_2-NH_2 by using low-toxic and cost-effective precursors. Take advantages of the magnetism, the magnetic adsorbent (Fe_3O_4@SiO_2-NH_2) shows a new application that treats dye pollutants. The optimum concentration of Fe_3O_4@SiO_2-NH_2 is 100 mg/L, while the initial concentration of malachite green is 10 mg/L at pH 7. The results indicate the removal of the malachite green is over 90%. The malachite green removal efficiency by Fe_3O_4@SiO_2-NH_2 is higher than that of Fe_3O_4@SiO_2. In addition, the adsorption capacity can be affected by ionic strength. The experimental data fits well with the Freundlich isotherm and the pseudo-second-order kinetic model. Real samples were treated and the experimental result shows that these real water samples had little interference. The Fe_3O_4@SiO_2-NH_2 nanoparticles as a magnetic adsorbent could be a promising future for environmental based process.

Acknowledgements

The authors would like to thank Kræftens Bekæmpelse and the Danish Research Council for Technology and Production (Grant 274-07-0172), Hubei Province Natural Science Fund Project (2014CFA080), Chutian Scholars Fund Project from the Education Department of Hubei Province, and Hundred Talents Program from the Organization Department of Hubei Province for financial support.

Notes and references

[a] School of Food and pharmaceutical Engineering, Key Laboratory of Fermentation Engineering (Ministry of Education), Hubei Provincial Cooperative Innovation Center of Industrial Fermentation, Hubei University of Technology, Wuhan 430068, China.
*Address correspondence to sunhonghao@mail.hbut.edu.cn.
Electronic Supplementary Information (ESI) See DOI: 10.1039/b000000x/

1 L. Ai, H. Huang, Z. Chen, X. Wei and J. Jiang, *Chem. Eng. J.*, 2010, 156, 243-249.
2 W. S. Wan Ngah, N. F. Md Ariff, A. Hashim and M. A. K. Megat Hanafiah, *Clean: Soil, Air, Water*, 2010, 38, 394-400.
3 C. A. Demarchi, M. Campos and C. A. Rodrigues, *J. Environ. Chem. Eng.*, 2013, 1, 1350-1358.
4 J. Wang, C. Zheng, S. Ding, H. Ma and Y. Ji, *Desalination*, 2011, 273, 285-291.
5 M. Vakili, M. Rafatullah, B. Salamatinia, A. Z. Abdullah, M. H. Ibrahim, K. B. Tan, Z. Gholami and P. Amouzgar, *Carbohydr. Polym.*, 2014, 113, 115-130.
6 V. K. Gupta, S. K. Srivastava and D. Mohan, *Ind. Eng. Chem. Res.*, 1997, 36, 2207-2218.
7 A. K. Sarkar, A. Pal, S. Ghorai, N. R. Mandre and S. Pal, *Carbohydr. Polym.*, 2014, 111, 108-115.
8 S. Nethaji, A. Sivasamy, G. Thennarasu and S. Saravanan, *J. Hazard. Mater.*, 2010, 181, 271-280.
9 A. Sergi, F. Shemirani, M. Alvandb and A. Tajbakhshian, *Anal. Methods*, 2014, 6, 7744-7751.
10 Y. C. Sharma, *J. Chem. Eng. Data*, 2011, 56, 478-484.
11 H. Tian, H. Wu, C. Hao, L. Du and Y. Fu, *Anal. Methods*, 2014, 6, 7703-7709.
12 R. Gopinathan, J. Kanhere and J. Banerjee, *Chemosphere*, 2015, 120, 637-644.
13 J. Wang, G. Zhao, Y. Li, H. Zhu, X. Peng and X. Gao, *Dalton Trans.*, 2014, 43, 11637-11645.
14 Y. F. Lin, H. W. Chen, C. C. Chang, W.C. Hungd and C. S. Chioud, *J. Chem. Technol. Biotechnol.*, 2011, 86, 1449-1456.
15 R. Mirzajani and S. Ahmadi, *J. Ind. Eng. Chem.*, 2014, DOI: org/10.1016/j.jiec.2014.08.011.
16 A. R´ıos, M. Zougaghbc and M. Bouriab, *Anal. Methods*, 2013, 5, 4558-4573.
17 A. Pourjavadi, S. H. Hosseini, F. Seidib and R. Soleymanc, *Polym Int.*, 2013, 62, 1038-1044.
18 M. Zhu and G. Diao, *Nanoscale*, 2011, 3, 2748-2767.
19 J. Liu, S. Z. Qiao, Q. H. Hu and G. Q. Lu, *Small*, 2011, 4, 425-443.
20 J. Lee, Y. Lee, J. K. Youn, H. B. Na, T. Yu, H. Kim, S. M. Lee, Y. M. Koo, J. H. Kwak, H. G. Park, H. N. Chang, M. Hwang, J. G. Park, J. Kim and T. Hyeon, *Small*, 2008, 1, 143-152.
21 M. A. Nasseri, B. Zakerinasaba and M. M. Samieadela, *RSC Adv.*, 2014, 4, 41753-41762.
22 R. R. Mishra, P. Chandran and S. S. Khan, *RSC Adv.*, 2014, 4, 51787-51793.
23 Y. J. Jin, F. Liu, M. Tong and Y. L. Hou, *J. Hazard. Mater.*, 2012, 227, 461-468.
24 B. Tian, T. Wang, R. Dong, S. Bao, F. Yang and J. Zhang, *Appl. Catal. B: Environ.*, 2014, 147, 22-28.
25 W. Stober, A. Fink and E. Bohn, *J. Colloid Interface Sci.*, 1968, 26, 62-69.
26 H. Sun, L. Cao and L. Lu, *Nano Res.*, 2011, 4(6), 550-562.
27 C. Shan, Z. Ma, M. Tong and J. Ni, *Water Res.*, 2015, 69, 252-260.
28 H. P. Cong, J. J. He, Y. Lu, S. H Yu, *Small*, 2009, 6, 169-173.
29 Y. Deng, D. Qi, C. Deng, X. Zhang and D. Zhao, *J. Am. Chem. Soc.*, 2008, 130, 28-29.
30 S. Zhan, Y. Yang, Z. Shen, J. Shan, Y. Li ,S. Yang and D. Zhu, *J. Hazard. Mater.*, 2014, 274, 115-123.
31 Y. S. Li, J. S. Church, A. L. Woodhead and F. Moussa F, *Spectrochim. Acta. A*, 2010, 76, 484-489.

32 R. K. Singh, T. H. Kim, K. D. Patel, J. C. Knowles and H. W. Kim, *J. Biomed. Mater. Res.A*, 2012, 100, 1734-1742.
33 H. Mittal, V. Parashar, S. B. Mishra and A. K. Mishra, *Chem. Eng. J.*, 2014, 255, 471-482.
34 S. Banerjee, M. C. Chattopadhyaya, V. Srivastava and Y. C. Sharma, *Environ. Prog. Sustain. Energy*, 2013, 3, 1-10.
35 R. K. Sheshdeh, M. R. K. Nikou, K. Badii and S. Mohammadzadeh, *Chem. Eng. Technol.*, 2013, 36, 1713-1720.
36 M. S. Derakhshan and O. Moradi, *J. Ind. Eng. Chem.,* 2014, 20, 3186-3194.
37 J. Zhang, Y. Li, C. Zhang and Y. Jing, *J. Hazard. Mater.,* 2008, 150, 774-782.
38 A. S. Sartape, A. M. Mandhare, V. V. Jadhav, P. D. Raut, M. A. Anuse and S. S. Kolekar, Arab. *J. Chem.,* 2014, DOI: org/10.1016/j.arabjc.2013.12.019.
39 A. Mohammadi, H. Daemi and M. Barikani, *Int. J. Biol. Macromol.,* 2014, 69, 447-455.
40 V. V. Kumar, S. Sivanesan and H. Cabana, *Sci. Total Environ.*, 2014, 487, 830-839.
41 G. Z. Kyzas, P. I. Siafaka, E. G. Pavlidou, K. J. Chrissafis and D. N. Bikiaris, *Chem. Eng. J.*, 2015, 259, 438-448.
42 B. Samiey and A. R. Toosi, *J. Hazard. Mater*., 2010, 184, 739-745.
43 A. K. Kushwaha, N. Gupta and M. C. Chattopadhyaya, *J. Saudi Chem. Soc.,* 2014, 18, 200-207.
44 M. K. Dahri, M. R. R. Kooh and L.B.L. Lim. *J. Environ. Chem.*, *Eng.,* 2014, 2, 1434-1444.
45 A. Pourjavadi, S. H. Hosseini, F. Seidib and R. Soleymanc, *Polym Int.*, 2013, 62, 1038-1044.

Graphical Abstract

Malachite green Adsorption onto Fe_3O_4@SiO_2-NH_2: Isotherms, Kinetic and Process Optimization

Ling Sun, Shuchao Hu, Hongmei Sun, Huiling Guo, Hongda Zhu, Mingxing Liu and Honghao Sun*

School of Food and pharmaceutical Engineering, Key Laboratory of Fermentation Engineering (Ministry of Education), Hubei Provincial Cooperative Innovation Center of Industrial Fermentation, Hubei University of Technology, Wuhan, 430068, China.

*Address correspondence to sunhonghao@mail.hbut.edu.cn.

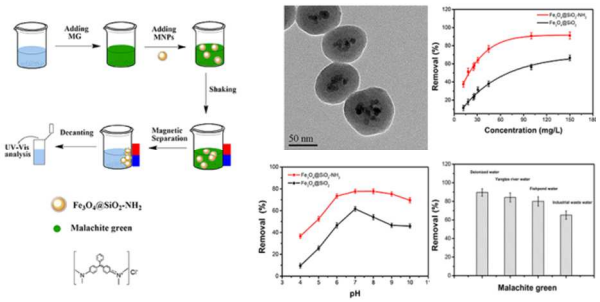

A novel magnetic adsorbent with an amino-modified SiO_2-coated Fe_3O_4 magnetite was prepared. Under the optimal conditions, the removal efficiency of malachite green is over 90% by the Fe_3O_4@SiO_2-NH_2.